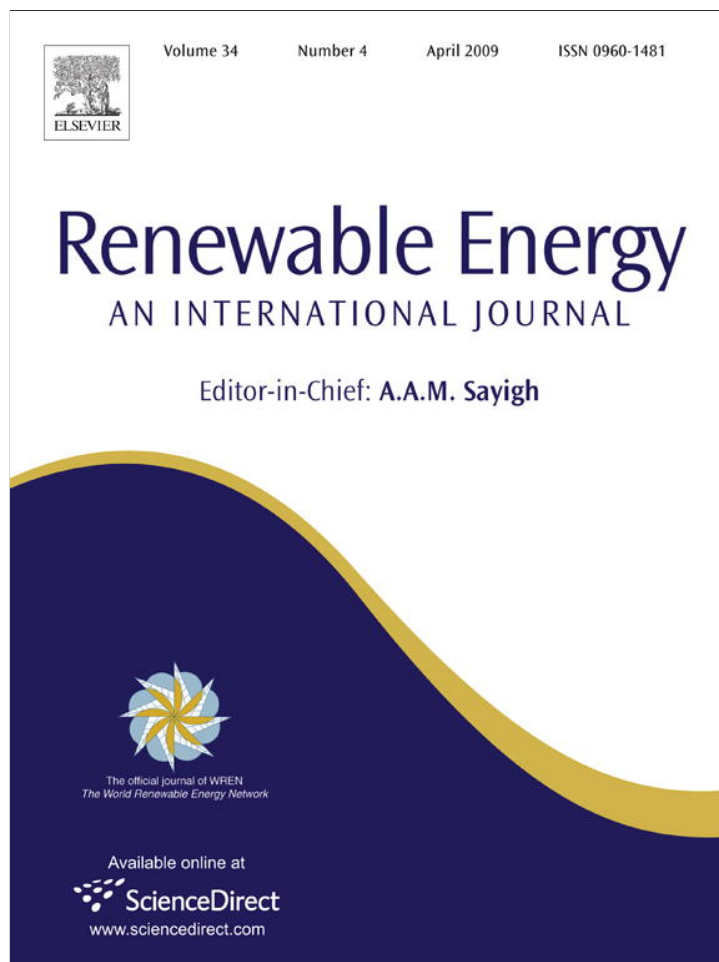


Provided for non-commercial research and education use.
Not for reproduction, distribution or commercial use.



This article appeared in a journal published by Elsevier. The attached copy is furnished to the author for internal non-commercial research and education use, including for instruction at the authors institution and sharing with colleagues.

Other uses, including reproduction and distribution, or selling or licensing copies, or posting to personal, institutional or third party websites are prohibited.

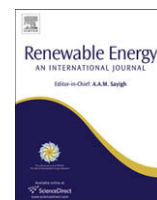
In most cases authors are permitted to post their version of the article (e.g. in Word or Tex form) to their personal website or institutional repository. Authors requiring further information regarding Elsevier's archiving and manuscript policies are encouraged to visit:

<http://www.elsevier.com/copyright>



Contents lists available at ScienceDirect

Renewable Energy

journal homepage: www.elsevier.com/locate/renene

Hot air balloon engine

Ian Edmonds*

Solartran Pty Ltd, 12 Lentara Street, Kenmore, Brisbane 4069, Australia

ARTICLE INFO

Article history:

Received 10 December 2007

Accepted 30 June 2008

Available online 16 August 2008

Keywords:

Solar power
Balloon engine
Solar tower
Hot air engine

ABSTRACT

This paper describes a solar powered reciprocating engine based on the use of a tethered hot air balloon fuelled by hot air from a glazed collector. The basic theory of the balloon engine is derived and used to predict the performance of engines in the 10 kW to 1 MW range. The engine can operate over several thousand metres altitude with thermal efficiencies higher than 5%. The engine thermal efficiency compares favorably with the efficiency of other engines, such as solar updraft towers, that also utilize the atmospheric temperature gradient but are limited by technical constraints to operate over a much lower altitude range. The increased efficiency allows the use of smaller area glazed collectors. Preliminary cost estimates suggest a lower \$/W installation cost than equivalent power output tower engines.

© 2008 Elsevier Ltd. All rights reserved.

1. Introduction

A near linear atmospheric temperature gradient extends from the Earth's surface to the tropopause. The change in temperature with height, known as the lapse rate, is $-0.65\text{ }^\circ\text{C}$ per hundred metres so that over the 10 km distance to the tropopause the temperature decreases from about $15\text{ }^\circ\text{C}$ to about $-50\text{ }^\circ\text{C}$. The temperature difference ($T_g - T_h$) between the high temperature source at ground level and a lower temperature sink some vertical height, h , above can be utilized to drive a heat engine. An example is the solar updraft tower or solar chimney. In this device a vertical tower is connected to a ground level glazed collector. Warm air from the glazed collector flows up through the tower and exits the tower at some height h above the ground. As the warm air in the tower is less dense than the ambient ground level air a pressure difference exists between the air at the bottom of the tower and the surrounding air. This pressure difference can be used to drive a turbine located at the bottom of the tower. The pressure difference across the turbine is maintained by warm air moving up the tower and a given parcel of warm air continues to generate power while it remains in the tower. It can be shown that the thermal efficiency of the solar updraft tower, $e = gh/(C_p T_g) = 34 \times 10^{-6} h$, where C_p is the specific heat of air and T_g is the ground level air temperature. The Carnot efficiency $(T_g - T_h)/T_g$ is implicit in this relation as, in the lower atmosphere, $T_g - T_h$ is proportional to h . A solar updraft tower built at Manzanares in Spain with a height of 195 m generated a peak output of 50 kW and cost about US\$1 million to build. The Manzanares tower thermal efficiency was

0.66%. The efficiency of the glazed collector at Manzanares was 33% and the air friction losses were about 50% so that the overall efficiency of the Manzanares power plant was about 0.1%. This low efficiency is primarily due to the fact that the Manzanares tower operated over only about 2% of the atmospheric temperature gradient and therefore operated between a temperature difference of only 1.3 ° . To obtain higher efficiencies the working height of an updraft tower must be increased. Proposed methods for increasing the working height include higher solar updraft towers [7], high downdraft towers [1], suspended membrane towers [6] and vortex towers [3]. The heights proposed for the updraft and downdraft towers (both 1000 m) would make these the tallest structures ever built. Currently none of these methods is being realized. This paper proposes a new type of solar engine that operates over several thousand metres height of the atmospheric temperature gradient.

2. Description of the balloon engine

A commercial hot air balloon envelope with a 44 m equivalent diameter is shown in Fig. 1. A windlass – generator/motor drive of the type that would be coupled to the balloon envelope is shown in Fig. 2. The four components of a balloon engine, a balloon envelope open at the bottom, a tethering rope, a windlass generator/motor drive and a glazed solar collector are illustrated in Fig. 3. At the start of a two stroke cycle the balloon is charged with hot air obtained by drawing ambient air through the glazed solar collector. The collector contains water filled tubes disposed perpendicularly to the air flow such that there is efficient heat transfer from the hot water in the tubes to the air. When the balloon is fully charged with hot air the windlass is released and, as the balloon ascends, the buoyancy force delivers mechanical power via the windlass to the generator/motor. During the upstroke the air in the balloon

* Tel./fax: +61 7 3378 6586.

E-mail address: ian@solartran.com.au



Fig. 1. The envelope of a Cameron Z-1600 hot air balloon. This balloon develops about 6 tonnes lift when charged with air at 60 °C.

expands adiabatically and cools, with some air continuously spilling from the bottom of the balloon throughout the upstroke. As the balloon ascends the density of air in the balloon approaches more closely to the density of the ambient air and the buoyancy of the balloon decreases. At some predetermined height a vent in the side of the balloon is opened by pressure sensitive means and a substantial fraction of the remaining warm air in the balloon is discharged. The generator/motor then switches to motor operation and the partly empty balloon is hauled down to ground level in



Fig. 2. A windlass coupled to a generator/motor of the type that would be used in a balloon engine.

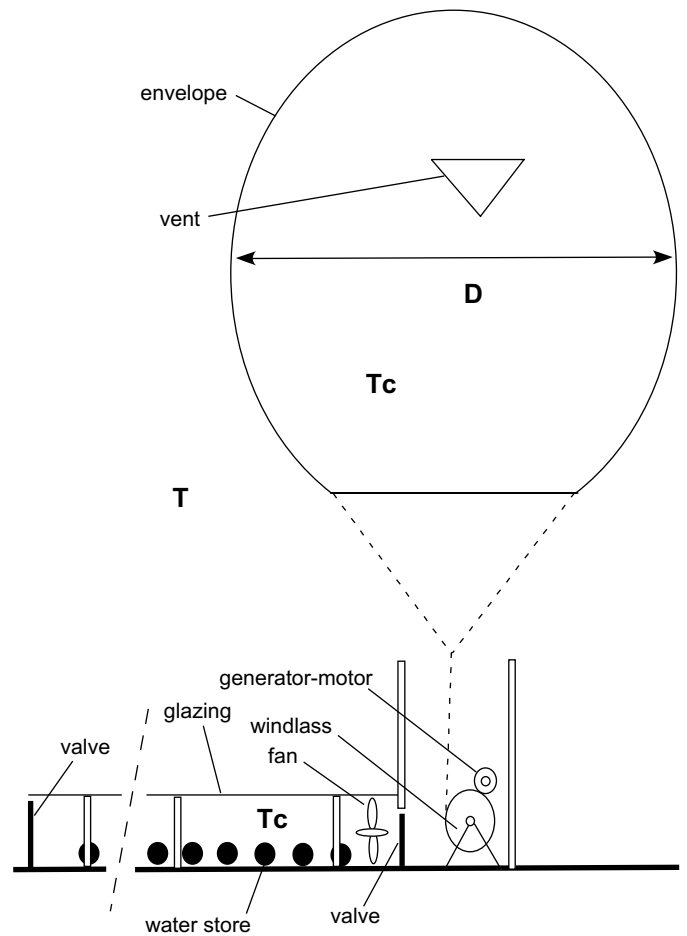


Fig. 3. The elements of a hot air balloon engine.

a down-stroke that completes the cycle. As the buoyancy force due to the balloon is larger on the upstroke than on the down-stroke a positive mechanical work output and a positive electrical output are obtained from the engine.

3. Theory of the balloon engine

The buoyancy force, F_b , experienced by a balloon of volume V is given by

$$F_b = Vg(\rho - \rho_i) - M_b g \quad (1)$$

where M_b is the mass of the balloon envelope, g is the gravitational acceleration and ρ and ρ_i is the density of air outside and inside the balloon, respectively. The outside air density varies with pressure, p , and temperature, T , and may be calculated from $\rho = pM/(RT)$. The molecular weight of dry air is $M = 0.02896$ kg/mol, the gas constant, $R = 8.3145$ J/(mol K) and the air temperature $T = T_0 + Lh$ where T_0 is the sea level air temperature and L is the temperature lapse rate, -0.065 K/m. The ambient air pressure at altitude h is given by $p = p_0(1 + Lh/T_0)^{-gM/RL}$ where p_0 is the sea level air pressure. Assuming adiabatic expansion and compression of the air in the balloon the temperature of the air in the balloon, T_i , is given by $T_i = T_c(p/p_0)^{(1-\gamma)/\gamma}$ where T_c is the temperature of the charge air and γ , the specific heat ratio for dry air, is 1.4. With these relations the buoyancy force on the balloon, F_b , as a function of altitude, h , may be found. The drive force at the windlass, F_d , is the difference between the buoyancy force and the weight of the tethering rope. $F_d = F_b - mgh$ where m is the mass per unit length of the tethering

rope. When the balloon is moving at velocity v a friction drag force exists and the drive force becomes

$$F_d = F_b - mgh \mp (1/2)C_d\rho Av^2 \quad (2)$$

where C_d is the drag coefficient ($C_d = 0.1$ for a smooth sphere) and A is the cross section area of the sphere.

4. Predicted performance of the balloon engine

The envelopes of practical hot air balloons are not spherical but more oblate spheroid at the top and conical at the bottom. However, the performance is not strongly dependent on the shape of the balloon and it is mathematically convenient to illustrate the practicality of the solar engine by calculating the performance of a spherical balloon envelope that approximates a commercially available hot air balloon envelope. The envelope used is a Cameron Z-1600 envelope, Fig. 1, enclosed volume $V = 45,300 \text{ m}^3$ (equivalent sphere diameter $D = 44 \text{ m}$) and envelope mass, $M_b = 513 \text{ kg}$. The envelope cost is A\$220,000 [4]. The tethering rope used is 1/2" diameter "Spectra" of breaking strain 85 kN and mass per unit length $m = 0.118 \text{ kg/m}$. The ambient ground air temperature is $T_0 = 15^\circ \text{C}$ and the charge air temperature is $T_c = 60^\circ \text{C}$. The balloon is constrained to ascend and descend at the constant rate of 5 m/s. The balloon generates power via the windlass and generator drive during the upstroke to a predetermined altitude of 6000 m. During the upstroke warm air spills from the bottom of the balloon as the air expands. At 6000 m altitude 40% of the air remaining in the envelope is discharged as a pressure sensitive vent opens. The balloon is then hauled in to ground level. The buoyancy force, F_b , and windlass drive force, F_d , calculated using Eqs. (1) and (2), are shown in Fig. 4 for the upstroke and the down-stroke phases of the cycle as a function of altitude. Notice that following air discharge at the top of the upstroke F_d decreases to a relatively small but positive force. The height at which discharge occurs is selected such that a substantial fraction of the remaining air can be discharged while maintaining a small positive tension force in the tethering rope so that the rope remains in tension throughout the cycle. The area between the upstroke and the down-stroke curves in Fig. 4 represents the work output of the engine. The calculated value is 144 MJ. The volume of air in the balloon at the end of the cycle is $15,500 \text{ m}^3$ and therefore the required recharge volume at the beginning of each cycle is $29,100 \text{ m}^3$. As the recharge air is raised in temperature from 15°C to 60°C the heat input to the engine is 1609 MJ. Thus the predicted thermal efficiency of the engine is $144/1609 = 0.089$ or about 9%.

With a constant upstroke and down-stroke velocity of 5 m/s the time for one cycle is 2400 s (40 min) and the average power output over the two stroke cycle is 60.0 kW. However, recharge time and recharge energy must be included as a third phase. Recharge with two 0.55 kW industrial fans each delivering $7.5 \text{ m}^3/\text{s}$ requires 1940 s. With recharge time and energy included the average power output over the three phases in each full cycle (72 min) is 33 kW.

From Fig. 4 it is evident that the work output diminishes with altitude and that it should be an advantage to operate the engine over a lower altitude range. Fig. 5 shows the buoyancy force and drive force for the same engine when the 80% discharge of remaining air occurs at 3000 m. The work output during upstroke and down-stroke of the engine is 124 MJ. The volume of air in the balloon at the end of the cycle is 6860 m^3 and therefore the required recharge volume at the beginning of each cycle is $37,700 \text{ m}^3$. As the recharge air is raised in temperature from 15°C to 60°C the heat input to the engine is 2090 MJ. Thus the predicted thermal efficiency of the engine is $124/2090 = 0.060$ or 6%.

With a constant upstroke and down-stroke velocity of 5 m/s the time for one cycle is 1200 s (20 min) and the average power output over the two stroke cycle is 103 kW. However, recharge time and

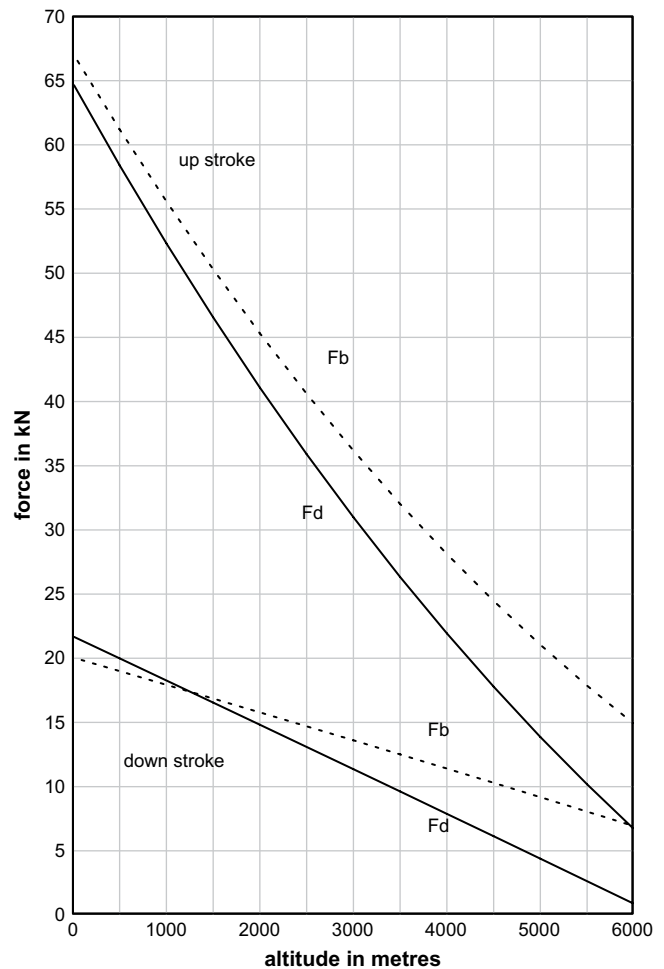


Fig. 4. The buoyancy force (dotted curve) and the drive force (full curve) for a 44 m diameter balloon during the cycle to 6000 m altitude and back; 40% discharge occurs at 6000 m altitude.

energy must be included. Recharge with four 0.55 kW industrial fans each delivering $7.5 \text{ m}^3/\text{s}$ requires 1256 s. With recharge time and energy included the average power output over the three phases in each cycle (41 min) is 51 kW.

The power output of a balloon engine scales as balloon diameter cubed. The envelope mass and the air friction losses scale as diameter squared. Therefore there should be significant benefits in larger scale systems. To illustrate the effect of scaling the envelope diameter is scaled up by a factor of two to 88 m. The envelope volume scales as D^3 up to $357,000 \text{ m}^3$ and the envelope mass as D^2 to 2050 kg. The tethering rope now requires seven strands of 1/2" diameter Spectra with a combined breaking strain of 560 kN (57 tonnes). The engine is again operated with 80% discharge of the remaining air at 3000 m altitude. The calculated buoyancy force, F_b , and windlass drive force, F_d , are shown in Fig. 6 for the upstroke and the down-stroke phase of the cycle as a function of altitude. The calculated work output per cycle is 1.014 GJ. The required recharge volume at the beginning of each cycle is $302,000 \text{ m}^3$. As the recharge air is raised in temperature from 15°C to 60°C the heat input to the engine is 16.7 GJ. Thus the thermal efficiency of the engine is $1.014/16.7 = 0.061$ or about 6%. Assuming a constant upstroke and down-stroke velocity of 5 m/s the time for the two stroke cycle is 1200 s (20 min) and the average power output over the two stroke cycle is 0.84 MW. Recharge by forty 0.55 kW fans each delivering $7.5 \text{ m}^3/\text{s}$ requires

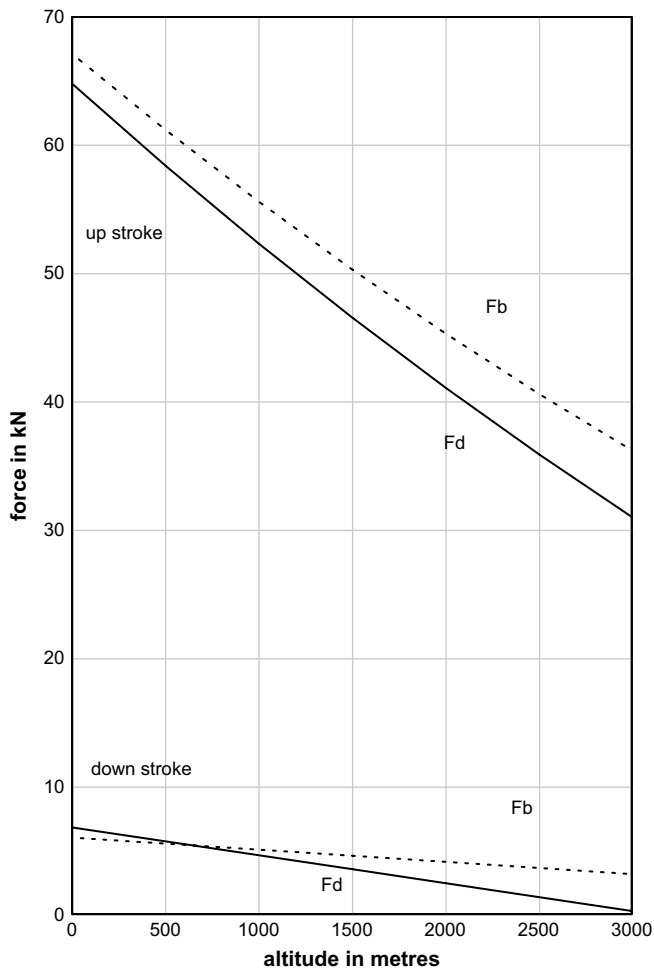


Fig. 5. The buoyancy force (dotted curve) and the drive force (full curve) for a 44 m diameter balloon during a cycle to 3000 m altitude and back; 80% discharge occurs at 3000 m altitude.

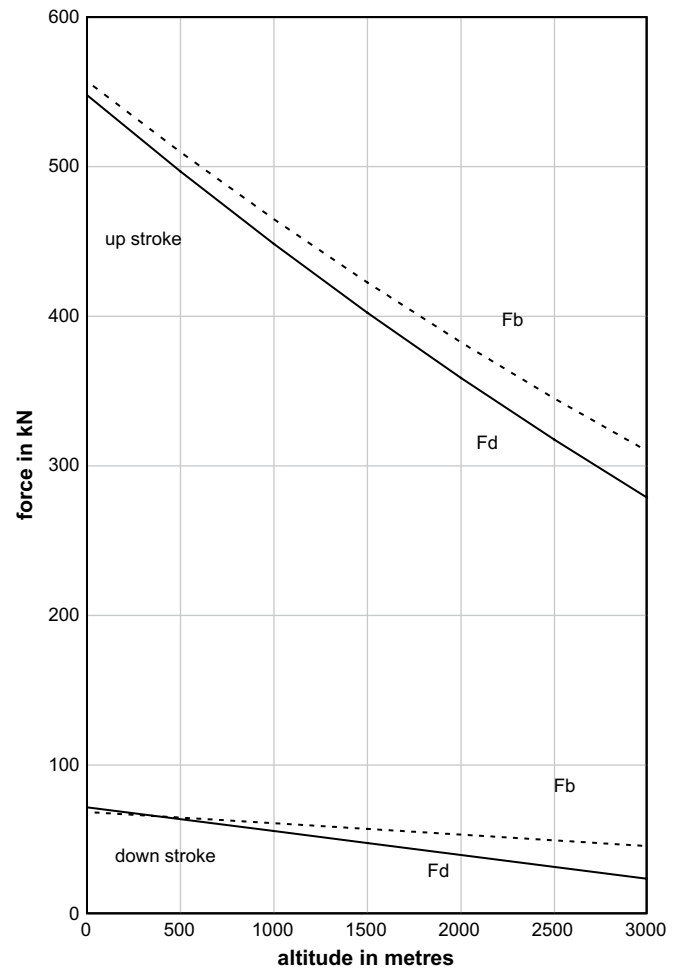


Fig. 6. The buoyancy force (dotted curve) and the drive force (full curve) for an 88 m diameter balloon during a cycle to 3000 m altitude and back; 80% discharge occurs at 3000 m altitude.

1006 s. Over the entire 37 min cycle including recharge the average power output is 0.47 MW.

The engines as described are parasitic on an external electrical supply to power the down-stroke. However, two engines operating in counter-phase and coupled mechanically or electrically (a double acting engine) would not require an external power supply.

5. Cost estimates

A first estimate cost may be obtained as follows. The retail cost of the Cameron Z-1600 envelope is A\$220,000. The envelope is made from a combination of heat resistant and rip-stop fabrics that may not be necessary in a balloon that does not carry passengers and is not heated by a propane burner. For example, solar balloons, deriving buoyancy entirely by solar radiation incident on the balloon envelope, are usually made from much less expensive polyethylene film [2]. Nevertheless the Z-1600 envelope cost is taken as indicative. Assuming the cost of the balloon envelope is one half the system cost with the collector, the windlass, the generator/motor and the 3000 m of 1/2" Spectra rope accounting for the other half of the system cost the overall projected cost is \$440,000. As the average power output over the cycle is 51 kW the system installation cost is \$9/W.

For the two times larger diameter system the envelope cost is assumed to scale as diameter squared to \$880,000 with, assuming the previous 50:50 split in system cost, the overall system cost

being \$1.76 million. The system cost per unit power output is \$1.76 M/0.47 MW = \$4/W.

6. Discussion

The very preliminary cost estimates suggest the installation cost of balloon engines would be similar in cost to other renewable energy technologies such as wind power and photovoltaic power. Both the balloon engine and the solar tower engines operate in the atmospheric temperature gradient. However, the thermal efficiency of the balloon is much higher as the engine can operate over several thousand metres while the solar tower is restricted by technical constraints to operate over several hundred metres. The predicted efficiencies of the 44 m and 88 m diameter, 3000 m altitude engines examined, 0.060 and 0.061, respectively, are about one half the efficiency predicted by the expression $gh/(C_p T_g)$ with $h = 3000$ m, 0.102. This is expected as the balloon engines discharge warm air progressively from ground level to the maximum height h and, at the maximum height, discharge only 80% of the enclosed air, the remainder returning to ground level in the balloon on the down-stroke. The principal benefit of the much higher efficiency is allowing a much smaller area and lower cost glazed collector than is the case with the solar updraft tower. The cost of a large glazed collector contributed to about half of the \$20/W cost of the Manzanares plant. A much smaller collector area requirement allows consideration of higher efficiency collection methods than

simple glazing over bare ground. It is envisaged that for this solar engine the glazed collector would incorporate an array of water filled tubes arranged perpendicular to the air flow direction. During the ascent/descent phase of the engine cycle the collector would be closed and the stored water would be heated by solar radiation to replace the heat transferred in the previous recharging. During recharge, ambient air would be drawn through the collector with heat convectively transferred from the water filled pipes to the air to provide a rapid recharge. This takes advantage of the high heat capacity of water to allow the large volume of recharge air to be supplied rapidly from a relatively small collector area. A first estimate of the size of the collector can be obtained as follows. For the 3000 m altitude engine based on the Z-1600 balloon (Fig. 5) the recharge rate with four fans each delivering $7.5 \text{ m}^3/\text{s}$ is $30 \text{ m}^3/\text{s}$. A collector with a cross section area of 6 m^2 will have an air velocity of 5 m/s through the collector. Assume the collector height is 0.5 m and the width is 12 m with the length to be found. Within the collector are water filled tubes of diameter 0.2 m and length 12 m disposed perpendicular to the length of the collector as in Fig. 7. During the 1200 s upstroke and down-stroke phase of the cycle the collector must absorb 2090 MJ of solar heat to provide the heat input during recharge. With sunlight of intensity $1 \text{ kW}/\text{m}^2$, and assuming all radiation absorbed, the required collector area is 1740 m^2 and the length of the 12 m wide collector is found to be 145 m . The number of water filled tubes required is $145/0.2 = 725$. The mass of water in each tube is 37.6 kg and the total mass of water is $27,260 \text{ kg}$. At the end of recharge when 2090 MJ has been transferred from the water to ambient air the average temperature decrease of the storage water is $18 \text{ }^\circ\text{C}$. The calculation of the temperature change of the water filled tubes within the collector as a function of time and distance through the collector is complicated. However, an intuitive estimate of the temperature changes is given in Fig. 7. The ambient air enters at $15 \text{ }^\circ\text{C}$ and exits at $60 \text{ }^\circ\text{C}$. The temperature of the input tube falls from $60 \text{ }^\circ\text{C}$ to $30 \text{ }^\circ\text{C}$ and the temperature of the exit tube falls from $80 \text{ }^\circ\text{C}$ to $70 \text{ }^\circ\text{C}$. With a linear temperature variation between input and exit, this would provide the required average temperature fall of $18 \text{ }^\circ\text{C}$. The average temperature difference between the air and the water filled tubes in the collector during recharge is, again from Fig. 7, $22.5 \text{ }^\circ\text{C}$. For air flow at 5 m/s across a storage cylinder of diameter 0.2 m the convective heat transfer coefficient is about $h = 30 \text{ W}/\text{m}^2\text{C}$. The combined surface area of the 725 tubes is 5466 m^2 . Thus the available convective heat transfer rate is $P = hA\Delta T = 30 \times 5466 \times 22.5 = 3.7 \text{ MW}$. During the 1256 s recharge time a total of 4647 MJ could be convectively transferred at this rate. This compares favorably with the 2090 MJ actually required for recharge. The estimate of 1740 m^2 area of glazed collector

required for this 51 kW solar engine is based on a collector efficiency of 100% . More realistically the collector efficiency may be 33% and the required collector area three times higher, about 6000 m^2 . However, this is still much less than the $45,000 \text{ m}^2$ area of glazed collector used in the 50 kW Manzanares plant. Finally an estimate of fan power to pump air at the rate of $30 \text{ m}^3/\text{s}$ through a 1740 m^2 glazed collector can be estimated by incorporating the friction effect of the storage tubes via a surface roughness term of 0.04 in the D'Arcy Weisbach equation for pressure drop. This yields a pressure drop of 88 Pa and a required fan power of 2.6 kW . This is roughly consistent with the fan power nominated for recharge in Section 4, (four industrial fans each of 0.55 kW with total fan power 2.2 kW).

A major assumption in the theory was adiabatic expansion of the balloon air during the upstroke and adiabatic compression during the down-stroke. Air-to-air heat transfer across a thin membrane is inefficient and, as the enclosed air mass is large, the percentage transfer of heat from the enclosed air mass to the ambient air is expected to be small during a cycle. Further, convective/radiative heat loss is expected to be substantially counter-balanced by radiant heat gain via the surface of the balloon if the balloon envelope is black. The mean temperature difference between the inside and the outside air during the cycle calculated to be $38 \text{ }^\circ\text{C}$. A preliminary heat transfer estimate for the 44 m balloon gives a convective rate of heat loss at the envelope of 0.85 MW and a rate of radiation from the envelope of 0.80 MW . A total rate of heat loss of 1.65 MW . Neglecting ground reflected sunlight, the rate at which radiant heat is incident on a 44 m diameter balloon in direct sunlight is 1.52 MW . This suggests a nett rate of heat loss of 0.13 MW . Over the 600 s of the upstroke the heat loss totals 78 MJ . This is much less than the 2090 MJ of heat added to the recharge air suggesting that the adiabatic assumption is reasonable. Measurements by Rochte [5] of internal and external air temperatures during a day long flight of a black solar balloon clearly demonstrated a nett thermal gain due to absorbed radiation.

Although the effect of wind on the operation of the engine has not been considered it is easy to show that wind would have a positive effect on power output. Nevertheless, it is envisaged that the solar engines would be used only at times of low wind, in particular during still, hot days in summer to supply the peak air conditioning loads that occur in Australia at these times. In this way a farm of balloon solar engines would complement a farm of wind turbines which would not be contributing power to the grid in these conditions. In principle this should allow a higher fraction of wind power to be incorporated in an electrical power grid before grid stability became a problem. At other times the envelopes of the solar engines would be stored in discharged state at ground level. This limited operation time is economically possible due to the relatively low infrastructure cost of this type of engine as compared with, for example, tower engines. The engine comprises a thin balloon envelope that, during operation, is self supported and a long length of rope. Both items are available from well established industries with competitive markets and both items are suitable for storage when not in use. Preliminary estimates suggest the glazed collector area required is at least an order of magnitude smaller in area than that required for an equivalent power output tower plant. The drive train of a balloon engine converts mechanical power to electrical power using a high torque, low frequency, rotating shaft via a gear train to a generator/motor similar in many respects to the drive train of a wind turbine. Much of the technology for wind turbines in the 10 kW to 1 MW range should be directly transferable to solar engines in the 10 kW to 1 MW range. Thus the windlass, drive train, generator/motor transducer may also be sourced from a well established industry. As Australia straddles the horse latitudes the wind resource is low and variable. Wind farms are mainly limited to a narrow strip around the Southern Australian

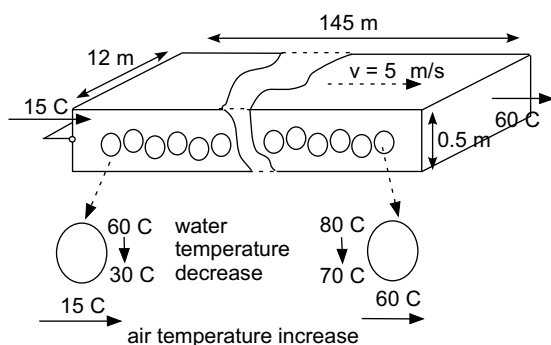


Fig. 7. An intuitive estimate of the average temperature changes of the air and water in a glazed solar collector during recharge of a balloon engine. Ambient air is heated, on average, from $15 \text{ }^\circ\text{C}$ to $60 \text{ }^\circ\text{C}$. Storage water at the inlet falls from $60 \text{ }^\circ\text{C}$ to $30 \text{ }^\circ\text{C}$ and storage water at the outlet falls from $80 \text{ }^\circ\text{C}$ to $70 \text{ }^\circ\text{C}$.

coastline; the rest of the continent has relatively low wind resources but high radiation resources. Within a future renewable energy mix balloon engines could complement wind turbines by providing grid power when the wind power is low. This should help to compensate for imbalance in the supply network due to the variability of wind power and allow for a higher ratio of wind power within the network.

The very preliminary cost estimates were based on actual and scaled costs of commercial hot air balloon envelopes. For these passenger carrying balloons specialized membranes are used for the envelopes. Solar balloons are usually made from lighter and less expensive polyethylene film, usually 10 μm film strips, taped or welded together to form the envelope, [2]. The envelope of the proposed solar engine could be made from polyethylene film. An 80 m long, 5 m wide roll of 100 μm black polythene film retails for A\$138; a material cost of \$0.345/m². A 44 m solar engine envelope has an area of 6082 square metres and a polyethylene film cost of A\$2100. Comparison with the A\$220,000 envelope cost used in the section on cost estimates suggests there is considerable scope for cost reduction by using less specialized membranes for the balloon envelope of the solar engine.

It is envisaged that a preliminary trial will utilize a Kavanagh C-56 envelope, the smallest commercial balloon envelope available in Australia. When charged to 60 °C this provides lift of about 180 kg and an average power output over the ascent and descent phases of about 4 kW.

7. Conclusion

A reciprocating balloon engine that operates over several thousand metres of the atmospheric temperature gradient has

been described. The engine is based on a balloon charged with hot air drawn from a glazed storage collector. The major components of the engine are derived from well established industries – the recreational hot air ballooning industry and the wind turbine industry. The elementary theory and basic mode of operation has been outlined. However, optimization of the operation mode and the electro-mechanical interface has not been considered. Indicative cost per installed watt based on commercially available balloon envelopes is about \$9/W. Scaling by a factor of two in balloon diameter would reduce the cost to \$4/W. The projected costs are comparable with other renewable technologies. However, there appears to be considerable scope to reduce the cost of the principal component, the balloon envelope. It is envisaged that the engines would be operated as summertime peak power supply units to complement wind turbine power.

References

- [1] Altmann T, Carmel Y, Guetta R, Zaslavsky D, Doytsher Y. Assessment of an "Energy tower" potential in Australia using a mathematical model and GIS. *Solar Energy* 2005;78:799–808.
- [2] Ballonsolaire. Available from: <http://perso.orange.fr/ballonsolaire/en-index.htm>; 2007.
- [3] Michaud LM. Vortex process for capturing the mechanical energy produced during upward heat convection in the atmosphere. *Applied Energy* 1999;62(4):241–51.
- [4] Purvis N. Private communication. Available from: <www.cameronballoons.com>; 2007.
- [5] Rochte R. Available from: <<http://mail.gpacademy.org/~rochter/>>; 2003.
- [6] Sorenson JO. Atmospheric thermal energy conversion utilizing inflatable pressurized rising conduit. US Patent 4,391,099; 1983..
- [7] Thomas MH, Davey RC. The solar tower: large scale renewable energy power station development. In: 19th World Energy Congress; Sydney, Australia; 2004.